ELECTROPHORETIC EFFECTS ON SATELLITE DROPLET FORMATION DURING ELECTROCOALESCENCE OF MICRODROPS

Rohit PILLAI[1*], **Joseph D. BERRY**[1 2†], **Dalton J. E. HARVIE**[1‡], **Malcolm R. DAVIDSON**[1§]

[1]Department of Chemical Engineering, University of Melbourne, AUSTRALIA

[2]CSIRO Mineral Resources Flagship, Melbourne, AUSTRALIA

[*] E-mail: r.pillai@student.unimelb.edu.au
[†] E-mail: joe.d.berry@gmail.com
[‡] E-mail: daltonh@unimelb.edu.au
[§] E-mail: m.davidson@unimelb.edu.au

ABSTRACT

Coalescence of charged drops in the presence of an electric field has practical applications in droplet based microfluidic devices. Existing studies have focused on macrodrops, but electrophoretic charge behaviour differs for microdrops. An electrokinetic model is used in this study to numerically investigate the charge transfer dynamics, for the problem of electrophoretic microdrop coalescence. In particular, the focus is on the formation of satellite droplets during partial coalescence, and the size and charge contained in them. It is found that the ionic conductivity (represented by dimensionless Debye length) determines whether the drop coalesces completely or partially, based on the relative importance of electrophoretic and capillary forces at coalescence. It is also shown that the size of the satellite droplet is sensitive to the initial separation distance, which affects the amount of charge separated at a partial coalescence event, and the associated electrophoretic force generated.

Keywords: CFD, droplet microfluidics, electrophoresis.

NOMENCLATURE

q	dimensionless charge density.
S	dimensionless initial separation distance.
K_d	dimensionless inverse Debye length.
$\boldsymbol{E}$	dimensionless electric field.
R_d	water drop radius, $[m]$.
$\boldsymbol{E}^*$	electric field, $[V/m]$.
T	absolute temperature, 298 $[K]$.
B	dimensionless parameter, $\rho_\mathrm{d} k^2 T^2 \varepsilon_0 \varepsilon_\mathrm{d} / 2 z^2 e^2 \mu_\mathrm{d}^2$.
k	Boltzmann constant, 1.38×10^{-23} $[m^2 kg/s^2 K]$.
e	elementary charge, 1.6×10^{-19} $[C]$.
$\boldsymbol{u}$	dimensionless fluid velocity.

Greek Symbols

ρ_w, ρ_o	density, $[kg/m^3]$.
μ_w, μ_o	viscosity, $[kg/ms]$.
ε_w, ε_o	permittivity, $[F/m]$.
ε_0	vacuum permittivity, $[F/m]$.
γ	interfacial tension, $[N/m]$.
α_+, α_-	diffusivity, $[m^2/s]$.
ρ	dimensionless density.
μ	dimensionless viscosity.
ε	dimensionless permittivity.
ϕ	VOF fractional volume function.
$\boldsymbol{\tau}_M$	dimensionless Maxwell electric stress tensor.
$\boldsymbol{\tau}_V$	dimensionless viscous stress tensor.

Latin Symbols

n_0	reference ion number density, $[m^{-3}]$.
n_+, n_-	species ion number density, dimensional $[m^{-3}]$, or dimensionless.
z_+, z_-	ion valency.
p	dimensionless pressure.

Subscripts

w	water phase.
o	oil phase.
$+$	cation.
$-$	anion.

Dimensionless Numbers

Re	Reynolds number.
We	Weber number.
Oh	Ohnesorge number.
Pe	Péclet number.
Ca	capillary number.

Acronyms

CCEP	contact charge electrophoresis.
CLSVOF	combined level set - volume of fluid.

INTRODUCTION

When an initially electroneutral drop comes into contact with an electrode, it acquires a net charge (Jung *et al.*, 2008). While the precise mechanism underlying contact charging has not yet been established (Im *et al.*, 2011), it is understood that the drop, post charging, is electrophoretically conducted away from the electrode. This phenomenon, known as Contact Charge Electrophoresis (CCEP) (Drews *et al.*, 2015), can be used to perform the precise drop manipulation required in microdrop based microfluidic devices. These devices treat each drop as a microreactor encapsulating a chemical/biological entity of interest (Theberge *et al.*, 2010), which is subsequently transported and analyzed. The contents of the drop are extracted by coalescing it into a bulk fluid (Fidalgo *et al.*, 2009). Hence the electrically induced coalescence of CCEP microdrops into a neutral bulk fluid is an important problem with practical applications. However, it has received scant attention in the CFD literature, in part

due to the complexities involved in modeling two-phase electrophoretic flow.

Surface energy arguments indicate that complete coalescence is energetically favored when an uncharged drop contacts a bulk fluid as it minimizes the total surface area. Sometimes, incomplete or partial coalescence can occur, resulting in a portion of the drop (called 'satellite droplet') pinching off. However, this is temporary as the satellite droplet subsequently proceeds to partially coalesce with the bulk fluid, producing a smaller droplet, and the process repeats until coalescence is completed (Thoroddsen and Takehara, 2000). When a charged drop is conducted towards a bulk fluid in the presence of an external electric field, electrohydrodynamic effects can induce a similar partial coalescence phenomenon (Hamlin *et al.*, 2012). Unlike the hydrodynamic case, however, the satellite droplet moves away from the interface (towards the top electrode) indicating that it has switched charge during the coalescence process. Despite the charge being transferred, remarkably, the size and charge of the satellite droplet was found to be independent of the ionic conductivity of the original charged drop. Instead, satellite droplet formation, at a fixed electric field, was understood to be a pure inertio-capillary process, with convection determining the quantity of charge transferred (Hamlin *et al.*, 2012). At high electric fields, charge transfer can be achieved without coalescence altogether, as the charge is conducted via a temporary meniscus bridge that connects the drops, and the drop appears to bounce off the interface (Bird *et al.*, 2009; Ristenpart *et al.*, 2009).

To date, the phenomenon of charged drop partial coalescence has been studied exclusively in the context of macroscale drops, where the charge can be assumed to be located entirely on the interfaces. However, charged microdrop dynamics differs in important ways from its macroscale counterpart, because the width of the space charge regions becomes significant in comparison to the drop size. Consequently, an electrokinetic model that accounts for the diffusive, conductive and advective transport of individual ion species, is needed to accurately capture the microdrop physics. Here, the electrophoretic partial coalescence of a charged microdrop into a neutral bulk fluid is studied, with a focus on the charge transfer process. In particular, we seek to shed light on the fundamental questions: when do satellite droplets form and what affects their size and charge?

MODEL DESCRIPTION

The model employs a Combined Level Set Volume of Fluid (CLSVOF) based electrokinetic implementation for two fluid flow with interfaces, which allows for the coupled calculation of convective, conductive, and diffusive ion transport, the electrical potential distribution, and the flow dynamics of the liquid phases. The transport of individual ions is considered, allowing for diffuse regions of non-uniform ion concentrations to arise, so that the conductivity distribution emerges as part of the calculation. Additional details about the model and its numerical implementation can be found in Berry *et al.* (2013)

Problem Setup

The system studied in this work is illustrated in figure 1. An axisymmetric, initially spherical water drop of undeformed radius R_d, is suspended in oil, as is common in microfluidic devices. A reservoir of bulk fluid (water, in this case) is located at a distance S below the drop. The outer fluid, oil, is a dielectric and does not contain ions. The bulk fluid, being initially electrically neutral but conducting, contains symmetric anions and cations with number densities n_+ and n_-, respectively, valencies $z_+ = -z_- = z$, and diffusivities $\alpha_+ = \alpha_- = \alpha$, and uniform initial ion number density n_0.

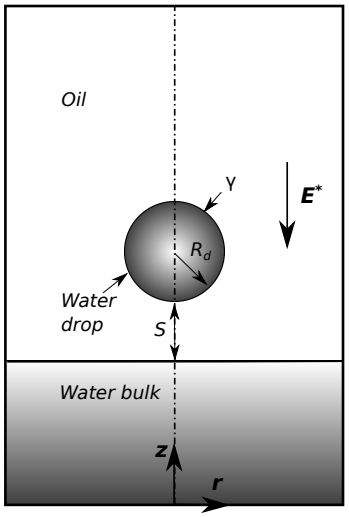

Figure 1: Schematic of an axisymmetric, charged drop of water (Symmetry boundary conditions are applied on the vertical centerline), suspended in oil, and acted on by an external electric field parallel to the z direction. The electric field electrophoretically conducts the drop towards the bulk fluid at the bottom of the domain.

The drop is assumed to have a net positive charge (physically achievable through direct contact with an electrode), which is implemented here by initializing it with a deficit of anions ($n_- = 0.95 \times n_+$), but is otherwise identical to the bulk fluid. Note that the water/oil interfaces are taken to be uncharged. A steady (DC) electric field $\boldsymbol{E}^*$ is imposed along the Z axial direction. The axial electric field is set up at the top and bottom boundaries to satisfy Gauss' law in the domain. Zero normal field conditions are specified on the side boundaries. As the drop is positively charged, it is conducted in the direction of the electric field, i.e. towards the bulk fluid. It is thus induced to coalesce into the bulk fluid.

The drop and bulk fluid are assumed to be symmetrical along the vertical centerline (as shown in figure 1), and the calculations are performed in cylindrical polar coordinates. The interface between the water and oil is assumed to have a constant interfacial tension γ. To simplify the problem, the phases are assumed to have equal permittivities ($\varepsilon_\mathrm{o} = \varepsilon_\mathrm{w}$), viscosities ($\mu_\mathrm{o} = \mu_\mathrm{w}$) and densities ($\rho_\mathrm{o} = \rho_\mathrm{w}$). Varying density has been shown to have little impact on drop deformation behaviour (Pillai *et al.*, 2014) while oils with viscosities close to that of water have been employed in microfluidic devices (Teh *et al.*, 2008). The unity permittivity ratio, while unphysical, allows us to isolate the effect of charge on coalescence, which is the focus of this study.

Governing Equations

The equations governing the flow, the electric field, and ion transport are rendered dimensionless by scaling the length, velocity, time, ions, and the electric field by R_d, γ/μ_w,

$\mu_w R_d/\gamma$, n_0 and kT/zeR_d, respectively. Here e is the elementary charge, k is the Boltzmann constant, and T denotes absolute temperature. The chosen velocity scale gives unity viscous capillary number, Ca = 1. The Ohnesorge number (Oh = $\sqrt{\text{We}}/\text{Re} = \mu_w/\sqrt{\rho_w R_d \gamma}$), which tends to be fixed for an experimental setup, is also taken to be unity. This corresponds to a drop of radius 1μm (typical for microfluidic devices), drop viscosity 10^{-3} Pa.s, drop density 10^3 kg/m^3, interfacial tension 1 mN/m. The external electric field has a fixed value of 1.7 kV/m. Oh = Ca = 1 implies that Re = We = 1 for all simulations conducted. The Péclet number (Pe) is 1000. The dimensionless equations are:

$$\nabla \cdot \boldsymbol{u} = 0, \quad (1)$$

$$\frac{\partial \rho \boldsymbol{u}}{\partial t} + \nabla \boldsymbol{.} (\rho \boldsymbol{u}\boldsymbol{u}) = -\nabla p + \frac{1}{\text{Re}} \nabla \boldsymbol{.} \boldsymbol{\tau}_V + \frac{1}{\text{We}} \boldsymbol{F}_S + \frac{2\text{B}}{\text{Re}^2} \boldsymbol{F}_E, \quad (2)$$

$$\frac{\partial c n_\pm}{\partial t} + \nabla \boldsymbol{.} (\boldsymbol{u} c n_\pm) = \frac{1}{\text{Pe}} \nabla \boldsymbol{.} (c \nabla n_\pm \mp c n_\pm \boldsymbol{E}), \quad (3)$$

$$\nabla \boldsymbol{.} (\varepsilon \boldsymbol{E}) = \frac{1}{2} K_d^2 q, \quad (4)$$

$$\frac{\partial \phi}{\partial t} + \nabla \boldsymbol{.} (\phi \boldsymbol{u}) = 0. \quad (5)$$

In equations (1-5) and hereafter, unsubscripted ρ, μ, ε, and n_+, n_- denote dimensionless quantities. Equation (5) is the transport equation for the disperse phase volume fraction. $\boldsymbol{u}$ is the fluid velocity vector, B is a dimensionless constant for water at a fixed temperature (Berry *et al.*, 2013), p is pressure, $\boldsymbol{E}$ is the electric field, $\boldsymbol{\tau_V}$ is the viscous stress tensor, $\boldsymbol{F}_S$ is the force due to the interfacial tension and ϕ is the fractional volume function of the disperse phase. Gravitational effects are minimal at the length scale studied, and are consequently neglected. $\boldsymbol{F}_E$ is the electrical force term acting on the drop (and the conducting bulk fluid), represented by the divergence of the Maxwell stress tensor,

$$\boldsymbol{F}_E = \nabla \boldsymbol{.} \boldsymbol{\tau}_M = \nabla \boldsymbol{.} [\varepsilon \boldsymbol{E}\boldsymbol{E} - \frac{1}{2} \varepsilon (\boldsymbol{E} \boldsymbol{.} \boldsymbol{E}) \boldsymbol{I}]. \quad (6)$$

In the case of phases with equal permittivities, this is equivalent to:

$$\boldsymbol{F}_E = \frac{1}{2} {K_d}^2 q \boldsymbol{E}. \quad (7)$$

Thus, the electric forces acting on the (conducting) disperse phase depend on $\boldsymbol{E}$, K_d and q, where q is the dimensionless charge density ($q = n_+ - n_-$), and K_d is the inverse dimensionless Debye length given as

$$K_d = \sqrt{\frac{2 z^2 e^2 n_0 R_d^2}{\varepsilon_0 \varepsilon_w k T}}. \quad (8)$$

Electrokinetic models predict the formation of a diffuse charge layer near an interface in the presence of an external electric field. This diffuse layer forms because the ion species are conducted to the opposite (top and bottom, in this case) interfaces of the drop. This results in an ion concentration gradient near the interface, which achieves equilibrium when conduction is balanced by diffusion. K_d^{-1} is a measure of the thickness of this diffuse layer, in relation to the characteristic length scale R_d. A high value of K_d implies a thin diffuse layer meaning that the charge is located in a small band adjacent to the interface. The right hand side of equation (8) shows that a higher K_d also implies a higher n_0 (when all other parameters are fixed). This translates to a higher initial ion concentration, or higher ionic conductivity. Therefore, K_d is associated with both the concentration and the location of ions in the drop.

RESULTS

Results are presented here for a charged drop coalescing into a bulk fluid for varying Debye length K_d and initial separation distance S. Based on the problem setup, the drop has an uniform initial value of dimensionless charge density $q = 0.05$, while $q = 0$ initially in the electroneutral bulk fluid.

Complete Coalescence

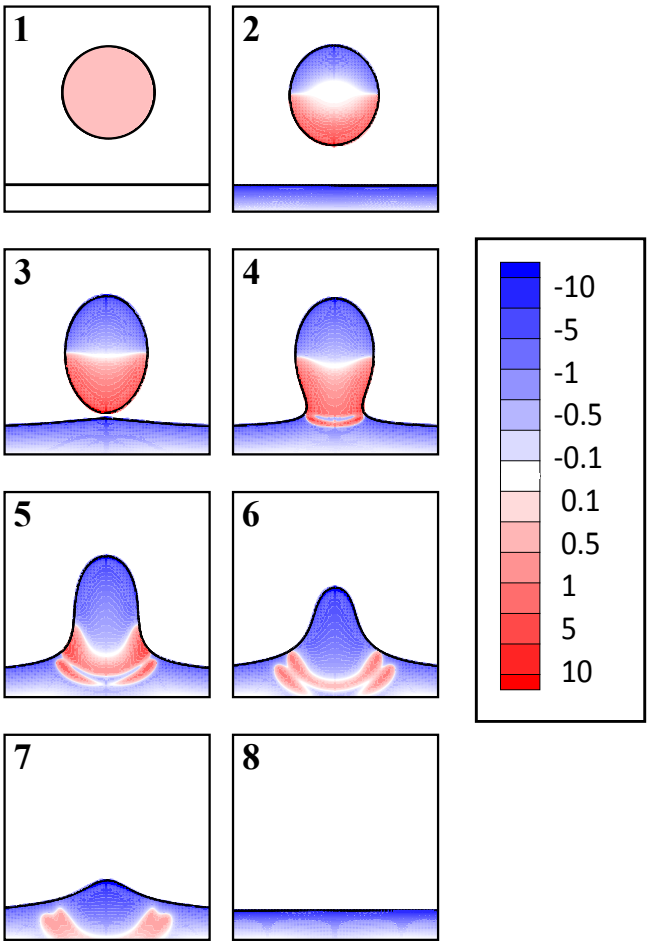

Figure 2: Left: Time lapse images (starting from top left) of a water drop ($S = 1$ and $K_d = 10$) undergoing complete coalescence, $t = 0, 2, 11.5, 12, 12.5, 13, 13.5, 22.5$. Right: Charge ($q$) contour scale for figures 2-5 (note logarithmic scale).

A complete coalescence case is studied in figure (2), where $S = 1$ and $K_d = 10$, with overlaid charge contours. The ions are present both inside the drop, and in the bulk phase. As both ion species are initially distributed equally and uniformly in the bulk fluid, to ensure electrical neutrality, it is colourless in the first frame. The drop, on the other hand, is positively charged, and the excess cations are also uniformly distributed. However, the electric field imparts equal but opposite conductive fluxes to each species (in both drop and bulk fluid) which results in anions migrating to one end and cations to the other. In the bulk fluid, depletion of cation species from the initially neutral region (just below the interface) leads to the formation of regions of negative charge (q) (frame 2). A symmetric region of positive charge also forms within the bulk fluid, at the lower boundary of the computational domain (not shown).

In the drop, the ions travel towards opposite ends of the drop, the regions of charge first develop at the drop tips, forming bands next to the upper and lower interfaces. The thickness of these bands depends on the choice of K_d. The electric field acts on the charged regions, resulting in a deforming electric force (equation 7) which stretches the drops as seen in the third frame. If the drop had been electroneutral, the regions of charge would continue to form at both ends, but the centre of the drop would stay stationary as it deformed (Pillai *et al.*, 2015). However, as the drop has a net charge, it moves and approaches the interface as it deforms (frame 3), and eventually makes contact with it (frame 4). Because the bulk surface and the approaching drop interface are oppositely charged, they experience an electrostatic attraction which lifts the bulk interface upwards prior to contact (frame 3).

In the absence of an electric field, a contacting drop - planar interface would take a finite time to coalesce, which would occur once the interfacial film of oil separating them had ruptured. But the electric field (and corresponding electrical force) accelerates the drainage of the oil film and the coalescence event happens effectively instantaneously, as seen in the transition from frames 3 and 4, half a time unit apart. At this point, the curvature of the electrophoretic drop is far greater than the bulk fluid ($R_d \ll R_{bulk}$). Hence, the capillary pressure inside the drop exceeds the corresponding value in the bulk by $2\gamma/R_d$. The analysis of Anilkumar *et al.* (1991) shows that the interfacial energy of the drop is of order $R_d^2\gamma$, and this energy is converted into kinetic energy of order $\rho_w R_d^3 u^2$ post interfacial film rupture, which facilitates the drop penetration into the bulk. When the two energies are equated, the velocity of the drop just after coalescence is estimated to be $u \simeq \sqrt{\gamma/\rho_w R_d} = 1$ m/s. For the case shown here, we measure velocities of ~ 0.5 m/s, which are significant. An interesting feature is the temporal development of the region of bulk phase surrounded by drop phase (first visible as a curved slit near the bottom of the drop in frame 4), which gradually leads to the separation of the drop charge into two narrow wavelike structures with large rounded ends (frames 6-7), prior to dissipation (frame 8).

Transition to Partial Coalescence

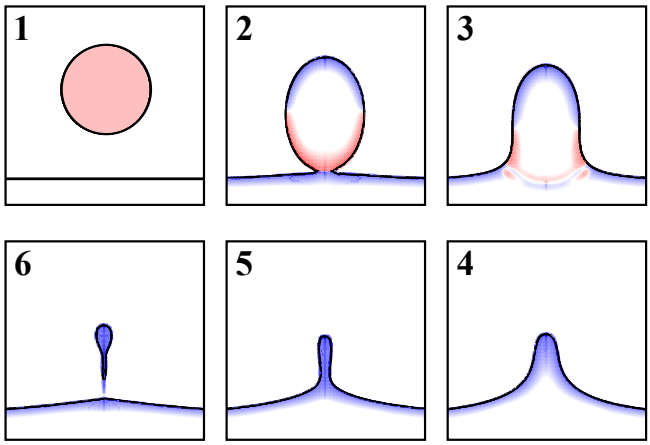

Figure 3: Time lapse images (clockwise, starting from top left) of a water drop ($S = 1$ and $K_d = 25$) undergoing partial coalescence, $t = 0, 3, 3.5, 4.5, 5, 5.5$. The overlaid charge contours employ the same scale as figure (2).

In figure (3), the coalescence process of a drop with higher ionic conductivity ($K_d = 25$), but the same separation distance ($S = 1$), is illustrated. The higher ionic conductivity, and hence the higher net charge on the drop, results in a larger electrophoretic force moving the drop, enabling it to reach the interface and coalesce into the bulk fluid faster (see t values in respective figure captions). The higher K_d also results in a narrower diffuse charge layer adjacent to the interface, plainly observable when comparing the cases (frame 2 of figure (3) against frame 3 of figure (2)). However, unlike the case in figure (2), the drop pinches off to form a satellite droplet, i.e. partial coalescence is observed (frame 6). This drop then moves vertically away from the interface (not shown here). The high velocity of drop penetration into the bulk begs the question as to why complete coalescence isn't observed here. The answer lies in the nuanced role interfacial tension plays in the coalescence process, along with the role of charge. In the absence of gravitational effects (as is the case here), the coalescence process is controlled by a competition between vertical and horizontal rates of collapse, both driven by interfacial tension. The vertically downward acting force, resulting from the capillary pressure difference between the drop and the bulk fluid outlined earlier, usually dominates over the inward horizontal acting force, driven by the azimuthal curvature of the neck. This means that the vertical collapse tends to prevail (as was the case in figure (2)), and the drop tends to coalesce into the bulk (Blanchette and Bigioni, 2006).

For the horizontal collapse to prevail, and pinch off of the droplet to occur, the vertical collapse must be sufficiently delayed by a suitable mechanism. For larger drops with sufficiently high interfacial tension ($Oh \leq 10^{-2}$), the convergence of capillary waves at the drop summit provide a suitable hydrodynamic mechanism (Blanchette and Bigioni, 2009). In the case studied here, with $Oh = 1$, this mechanism is absent. As such, upon application of an external electric field, it is the electrophoretic lift force generated by the negative charge near the upper drop interface, interacting with the downward electric field, that acts as a delaying electrohydrodynamic mechanism. While the positive charge at the lower interface is convected into the bulk fluid (frames 2-3), the influence of the near-symmetric negative charge formed at the upper drop interface opposes this convective fluid drainage into the bulk, delays it until horizontal collapse occurs, resulting in the formation of a satellite droplet. This satellite droplet is subsequently electrophoretically conducted away from the interface, indicating the switch in net charge from positive to negative. The coalescence process can therefore be understood as a competition between the electrophoretic force acting upward at the top of the drop and the capillary force acting downward. Therefore, charged drops coalesce completely below a critical ionic conductivity (figure (2), lower electrophoretic lift force), and partially above it (figure (3), higher electrophoretic lift force). This understanding is consistent with the study of Hamlin *et al.* (2012), who found a similar critical ionic conductivity separating regimes of partial coalescence (lower electrophoretic lift force), and non-coalescence or 'bouncing' (higher electrophoretic lift force).

In figure (4), the coalescence process of a drop with a larger initial separation distance ($S = 3$) for the same ionic conductivity as the case in figure (3) ($K_d = 25$), is illustrated.

This represents a drop that has contacted the electrode further away, and consequently undergoes CCEP over a longer distance before contacting the bulk fluid interface. The first three frames appear superficially similar to the corresponding ones in figure (3) (the times are selected in order to allow for a convenient comparison). However, on closer examination of the third frame of both figures, the peak of the drop appears to be higher (figure (4)) compared to the last case (figure(3)). This implies that the drop has undergone greater deformation than the case in figure (3), as would be expected from the fact that the drop was deforming for a longer period of time owing to its greater distance from the bulk interface. The bottom frames (4-6) in figure (4) depart significantly from the corresponding frames in figure (3). The drop summit is higher (frames 4-5) and the satellite droplet formed is larger (frame 6). This differs from the findings of Hamlin *et al.* (2012) who, while experimentally studying macroscale drop coalescence, found that the size and charge of satellite droplets is independent of all physical parameters, for a fixed value of electric field. As the electric field is fixed for all the simulations in this work, this phenomenon does not yield an obvious explanation.

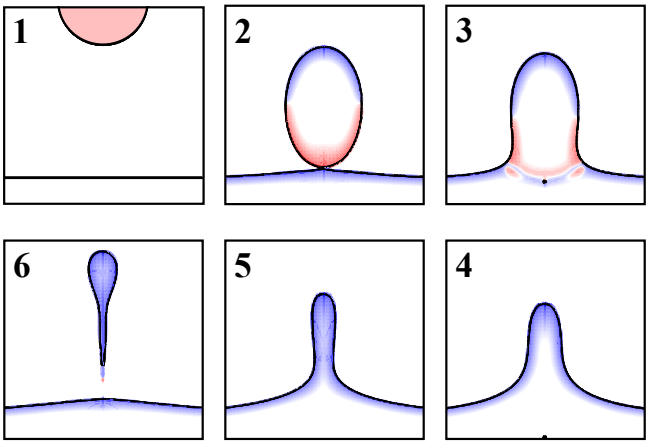

Figure 4: Time lapse images (clockwise, starting from top left) of a water drop ($S = 3$ and $K_d = 25$) undergoing partial coalescence, $t = 0, 9, 9.5, 10.5, 11, 12$. The overlaid charge contours employ the same scale as figure (2).

Satellite Droplet Characteristics

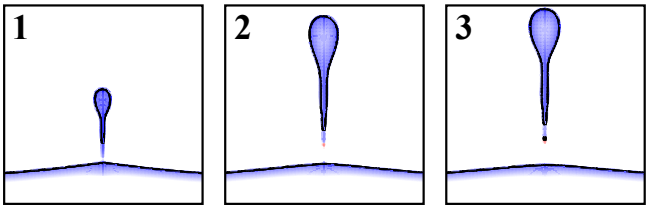

Figure 5: Satellite droplet comparison for $K_d = 25$, for three separation distances $(1)S = 1$, $(2)S = 3$ and $(3)S = 5$.

To probe the above apparent inconsistency further, the satellite droplets for three cases with different separation distances ($S = 1, 3$ and 5, respectively) has been shown in figure (5), for the same ionic conductivity $K_d = 25$. The significant variation between the first two frames, noted earlier, can be directly compared. However, increasing the separation distance additionally by the same amount (frame 3), does not result in a similar increase in droplet size, though the bulb of the drop is still slightly bigger when compared to $S = 3$ case (frame 2). The charge measurements of the three satellite droplets are consistent with the expectation that charge and volume (of satellite droplets) are roughly proportional (Pillai *et al.*, 2015). The charge contained in the satellite droplet increases significantly from $S = 1$ to $S = 3$, but a much smaller difference is observed for a commensurate increase of separation distance to $S = 5$. This indicates that the physical process controlling the satellite droplet size changes with separation distance (S), but asymptotes to a near constant value relatively quickly as S increases.

A possible explanation can be proposed for this phenomenon, arising from the differences between the charge separation dynamics, and consequent charge transfer dynamics, of macroscale and microscale drops. In the case of macroscale drops, diffuse space charge layers adjacent to the interface are infinitesimally thin, and the charge can be assumed to be completely located at the interface (Saville, 1997). In this case, as the macrodrop approaches the interface, the positive charge is practically located entirely at the lower, or leading, drop interface. Similarly, the negative charge is located entirely at the upper, or trailing drop interface. When the drop contacts the interface of the bulk fluid, the entire positive charge is almost instantaneously transferred, while the entire negative charge is contributing to the electrophoretic lift force at the drop summit. In this system, the actual pinching-off process is entirely interfacial tension driven, with charge dynamics not varying when the drop separation distance is varied. Consequently, the size and charge of satellite droplets would be independent of all physical parameters (ionic conductivity, separation distance) for a fixed setup (constant interfacial tension and electric field).

However, the high surface-to-volume ratios of microdrops means that the ratio of space charge layers to the drop radius (R_d) is higher, and the diffuse charge occupies a significant region adjacent to the drop interface (these diffuse layers can be observed in figures (2)-(4)). Which is to say that K_d, which is related to the diffuse layer thickness, has a finite value for microdrops ($K_d \to \infty$ for macrodrops). Unlike for macrodrops, the charge separation process (and diffuse layer formation process) is more complicated in microdrops. The electric field creates regions of charge by conducting the ion species away from the opposite ends. This process is not instantaneous, and has an associated timescale (Pillai *et al.*, 2015). Consequently, the drop may not necessarily be in steady state when it contacts the interface, as the equilibrium between conductive and diffusive fluxes inside the drop might not have been achieved. The ongoing charge separation dynamics post coalescence can result in ongoing charge transfer dynamics post coalescence. This means that all the positive charge is not instantaneously transferred out of the leading end, and the negative charge driven electrophoretic lift force is not constant at the trailing interface, post coalescence.

Using this understanding of microdrop charge behavior, the variation in satellite droplet size and charge can result from separation distance dependent charge transfer. The time lag associated with charge separation means that the closer the initial location of the drop is to the bulk fluid, the less likely it is to achieve steady state diffuse layer

equilibrium prior to coalescence. This means that the lower the separation distance, the greater the possibility of charge separation occurring post coalescence. This would result in a lower electrophoretic lift force at the top of the drop (as it is proportional to charge formation), and consequently, greater capillary pressure driven convection into the bulk prior to horizontal collapse. This process would then culminate in the pinching off of a smaller satellite droplet, as a greater proportion of the drop volume is convected into the bulk fluid. This explains how the size and charge of satellite droplets are lower for smaller separation distances, indicating that the size of the satellite droplet ejected by macrodrops is probably represented by the limiting case of high K_d, rather than a self-similar physical phenomenon as suggested by Hamlin *et al.* (2012).

CONCLUSIONS

The coalescence of a charged microdrop undergoing Contact Charge Electrophoresis (CCEP) (Drews *et al.*, 2015) with a electroneutral bulk fluid, is studied in this work. The drop interface is assumed to be uncharged, with the charge arising from an initial imbalance in the ion species uniformly distributed in the drop. The effect of varying ionic conductivity (K_d) and initial separation distance (S) on the coalescence process is explored. First, the transition from complete coalescence, where the drop completely enters the bulk, to partial coalescence, where a portion of the drop pinches off as a satellite droplet, is studied. It is shown that there is a critical drop ionic conductivity separating the two regimes, analogous to the limit reported by Hamlin *et al.* (2012), between the partial coalescence and the non coalescence (or 'bouncing') regimes. This results from the competition between the downward acting capillary pressure driven convection and an upward acting electrophoretic lift force. For higher ionic conductivities, the proportionally higher electrophoretic lift force is able to delay the capillary drop fluid drainage long enough for a satellite droplet to be pinched off.

Second, it is observed that the satellite droplet size and charge increases with initial separation distance, but this effect diminishes at higher separation distances. This result is explained as resulting from the distinct charge separation dynamics, and consequent charge transfer dynamics, of microdrops. In particular, the time lag associated with charge separation in microdrops implies that the closer the drop is initially to the bulk fluid, the less likely it is to achieve steady state deformation and associated steady state charge separation. This results in a lower electrophoretic lift force post coalescence, which allows the competing convective flow to drain more drop fluid into the bulk before the horizontal interfacial tension driven collapse pinches off a (smaller) satellite droplet.

This study can be extended in various interesting ways. The partial and complete coalescence regimes can be delineated in further detail, with the aid of parameter phase maps and scaling laws. The higher electric field non-coalescence regime can also be studied. The restriction on physical and electrical parameters can be relaxed, allowing for studying more realistic water-in-oil scenarios. The algorithm used in this work has recently been extended to include interface charge (Davidson *et al.*, 2014), which adds a layer of complexity to this problem, and will be employed in future work.

ACKNOWLEDGEMENTS

One of the authors (R. Pillai) acknowledges the support of a Melbourne International Research Scholarship (MIRS) during the completion of this work.

REFERENCES

ANILKUMAR, A.V. *et al.* (1991). "Surface-tension-induced mixing following coalescence of initially stationary drops". *Physics of Fluids A: Fluid Dynamics*, **3**, 2587–2591.

BERRY, J. *et al.* (2013). "A multiphase electrokinetic flow model for electrolytes with liquid/liquid interfaces". *Journal of Computational Physics*, **251**, 209–222.

BIRD, J. *et al.* (2009). "Critical Angle for Electrically Driven Coalescence of Two Conical Droplets". *Physical Review Letters*, **103(16)**, 164502.

BLANCHETTE, F. and BIGIONI, T.P. (2006). "Partial coalescence of drops at liquid interfaces". *Nature Physics*, **2(4)**, 254–257.

BLANCHETTE, F. and BIGIONI, T.P. (2009). "Dynamics of drop coalescence at fluid interfaces". *Journal of Fluid Mechanics*, **620**, 333.

DAVIDSON, M.R. *et al.* (2014). "Numerical simulation of the deformation of charged drops of electrolyte". *Advances in Fluid Mechanics X, WIT Press*, vol. 82, 203–214.

DREWS, A.M. *et al.* (2015). "Contact Charge Electrophoresis: Experiment and Theory". *Langmuir*, **31(13)**, 3808–14.

FIDALGO, L.M. *et al.* (2009). "Coupling microdroplet microreactors with mass spectrometry: reading the contents of single droplets online." *Angewandte Chemie*, **48(20)**, 3665–8.

HAMLIN, B.S. *et al.* (2012). "Electrically tunable partial coalescence of oppositely charged drops". *Physical Review Letters*, **109(9)**, 094501.

IM, D.J. *et al.* (2011). "Electrophoresis of a charged droplet in a dielectric liquid for droplet actuation". *Analytical Chemistry*, **83(13)**, 5168–5174.

JUNG, Y.M. *et al.* (2008). "Electrical charging of a conducting water droplet in a dielectric fluid on the electrode surface". *Journal of Colloid and Interface Science*, **322(2)**, 617–623.

PILLAI, R. *et al.* (2014). "Effect of interfacial tension and electric field on charge separation dynamics inside stable and unstable microdrops". *19th Australasian Fluid Mechanics Conference*, December, 8–11.

PILLAI, R. *et al.* (2015). "Electrolytic drops in an electric field: A numerical study of drop deformation and breakup". *Physical Review E*, **92(1)**, 013007.

RISTENPART, W.D. *et al.* (2009). "Non-coalescence of oppositely charged drops." *Nature*, **461(7262)**, 377–80.

SAVILLE, D. (1997). "Electrohydrodynamics: the Taylor-Melcher leaky dielectric model". *Annual review of fluid mechanics*, **(1962)**, 27–64.

TEH, S.Y. *et al.* (2008). "Droplet microfluidics." *Lab on a chip*, **8(2)**, 198–220.

THEBERGE, A.B. *et al.* (2010). "Microdroplets in microfluidics: an evolving platform for discoveries in chemistry and biology." *Angewandte Chemie*, **49(34)**, 5846–68.

THORODDSEN, S.T. and TAKEHARA, K. (2000). "The coalescence cascade of a drop". *Physics of Fluids*, **12(6)**, 1265.